

Contents lists available at [SciVerse ScienceDirect](http://www.sciencedirect.com)

Radiation Measurements

journal homepage: www.elsevier.com/locate/radmeas

Boron thin films and CR-39 detectors in BNCT: A method to measure the $^{10}\text{B}(n,\alpha)^7\text{Li}$ reaction rate

B. Smilgys^a, S. Guedes^a, M. Morales^b, F. Alvarez^b, J.C. Hadler^{a,*}, P.R.P. Coelho^c, P.T.D. Siqueira^c, I. Alencar^a, C.J. Soares^a, E.A.C. Curvo^d

^a Departamento de Raios C3smicos e Cronologia, Instituto de F3sica "Gleb Wataghin", UNICAMP, 13083-970 Campinas, SP, Brazil

^b Departamento de F3sica Aplicada, Instituto de F3sica "Gleb Wataghin", UNICAMP, Campinas, SP, Brazil

^c Centro de Engenharia Nuclear, Instituto de Pesquisas Energ3ticas e Nucleares, CNEN, S3o Paulo, SP, Brazil

^d Instituto de F3sica, UFMT, Cuiab3, MT, Brazil

H I G H L I G H T S

- ▶ Homogeneous boron thin films were successfully deposited using the sputtering technique.
- ▶ Boron thin films allow for the direct measurement of the $^{10}\text{B}(n,\alpha)^7\text{Li}$ reaction rate.
- ▶ CR-39 was calibrated for the evaluation of fast neutron contribution in BNCT irradiations.

A R T I C L E I N F O

Article history:

Received 9 December 2011

Received in revised form

4 June 2012

Accepted 5 July 2012

Keywords:

BNCT

Boron thin films

CR-39

Neutron dosimetry

A B S T R A C T

The working principle of the Boron Neutron Capture Therapy (BNCT) is the selective delivery of a greater amount of boron to the tumor cells than to the healthy ones, followed by the neutron irradiation that will induce the emission of α -particles and recoil ^7Li nuclei through the $^{10}\text{B}(n,\alpha)^7\text{Li}$ reaction. The objective of this work is to present a setup composed of a boron thin film coupled with CR-39. Alpha and ^7Li particle coming from the boron films are used to quantify neutron boron reaction and are detected by CR-39. The nuclei compounding of this detector, H, C and O, will undergo fast neutrons reactions, which will be detected in the CR-39 itself. In this way, the $^{10}\text{B}(n,\alpha)^7\text{Li}$ reaction and the contribution of fast neutrons to the flux can be determined at the same time. These measurements are essential for treatment planning as well as for studies of the biodistribution of ^{10}B -carrier drugs and tissue microdosimetry. The boron films were deposited on stainless steel substrates through the sputtering technique and irradiated with thermal neutrons at the reactor IEA-R1 located at IPEN, S3o Paulo/SP, Brazil. Here we show the first results on the characterization of these thin films and calibration of the proposed setup.

© 2012 Elsevier Ltd. All rights reserved.

1. Introduction

Ideally, cancer treatments should selectively destroy the tumor cells causing minimum damage to the healthy tissue. Aiming this goal, a therapy based on the reaction of low energy neutron capture by ^{10}B (a stable boron isotope), the *Boron Neutron Capture Therapy* (BNCT), is being researched worldwide. BNCT is a binary radiotherapy that consists in injecting boron into the tissue and then exposing it to thermal neutron irradiation (incident neutrons with energy less than 0.5 eV). When ^{10}B captures thermal neutrons, it decays into an α -particle (1.47 MeV) and ^7Li ion (0.84 MeV), both

with high linear energy transfer ($\text{LET}_\alpha \sim 190 \text{ keV}/\mu\text{m}$ and $\text{LET}_{\text{Li}} \sim 160 \text{ keV}/\mu\text{m}$), and their combined ranges are in the magnitude of a typical cell diameter ($\sim 12 \mu\text{m}$). Therefore, if there is a higher concentration of ^{10}B in the tumor cells, the damage caused by this nuclear reaction will be greater to the cancer than to the healthy tissue. To an effective BNCT, boron concentration in tumor should be of about $20 \mu\text{g}/\text{g}$ and the tumor/healthy tissue and tumor/blood boron concentration ratios should be about 3–4:1 (Coderre and Morris, 1999; Barth et al., 2005). It has been proven that BNCT can be efficient for the treatment of inoperable tumors or those which already present metastases (Altieri et al., 2008).

When irradiating a tissue containing boron with neutrons, while the main contribution to the dose comes from the $^{10}\text{B}(n,\alpha)^7\text{Li}$ reaction, the interactions of thermal neutron with nitrogen, $^{14}\text{N}(n,p)^{14}\text{C}$, which results in 590 keV proton, and the interactions of

* Corresponding author. Tel.: +55 19 35215316; fax: +55 19 35215512.

E-mail address: hadler@ifi.unicamp.br (J.C. Hadler).

epithermal ($0.5 \text{ eV} < E_{\text{neutron}} < 10 \text{ keV}$) and fast ($E_{\text{neutron}} > 10 \text{ keV}$) neutrons with hydrogen, carbon and nitrogen must be considered when calculating the effective dose delivered to the patient. This is because although the boron cross section for thermal neutron capture is much higher than the other reaction cross sections, the concentrations of hydrogen, carbon and nitrogen in tissues are also much higher than the boron concentration. Ideally, neutron beams in BNCT facilities should deliver only epithermal neutrons for the treatment of deep tumors or only thermal neutrons for cell culture experiments and the treatment of shallow tumors as melanoma. However, it is common to have a contamination of epithermal and fast neutrons which will interact with tissues, mainly by scattering processes.

The solid state nuclear track detector (SSNTD) CR-39, with composition $\text{C}_{12}\text{H}_{18}\text{O}_7$, can be used both as a tissue equivalent material for fast neutron microdosimetry (Durham et al., 1989; Deevband et al., 2011), since it has almost the same tissue composition (Table 1) and, after proper calibration, to monitor the fast neutron fluence. The SSNTDs record the passage of charged particles permanently and the region around the charged particle's path is more reactive to chemical etching agents, which makes possible to reveal the particle tracks and observe them at optical microscopes. The track size is related to the energy and mass of the incident particles.

The main goal of this work is the precise measurement of the $^{10}\text{B}(n,\alpha)^7\text{Li}$ reaction rate, necessary for treatment planning and biodistribution and dosimetric studies. For this, we propose a setup composed of a boron thin film (i.e. thickness much less than the α and ^7Li ranges) coupled with a sheet of CR-39 (Fig. 1). CR-39 is used to detect α -particles and ^7Li tracks from the film (neutron converter).

On the other hand, CR-39 itself is a fast neutron converter and, then, at the same time detector for the fast neutron reactions. In this way, it is possible to evaluate the contribution of fast neutrons (counting tracks in the non coupled side of the CR-39, background tracks) and to measure the $^{10}\text{B}(n,\alpha)^7\text{Li}$ reaction rate (counting tracks in the side of CR-39 coupled to the film and discounting the background).

2. Methodology

In a previous work, we tested the manufacturing of boron thin films using the *Chemical Solution Deposition* (CSD) method (Smilgys et al., 2011). Here, we show the results for other method of thin film manufacturing, the *Physical Vapor Deposition* (PVD). This latter method is tested with the aim of obtaining thinner and more homogeneous boron films.

Sputtering, a PVD method, is a process commonly used for thin film deposition, which consists in bombarding a target with energetic particles and provoke the ejection of atoms from the target (Behrisch, 1981). For manufacturing thin films, these ejected atoms from the target are deposited onto a substrate. We used a 99.9% pure boron target that was bombarded by an argon beam (of $\sim 1400 \text{ eV}$ and flow $\sim 7.5 \text{ sc cm}$) and deposited onto stainless steel substrates 316 L (at $\sim 350 \text{ }^\circ\text{C}$) at the *Laboratório de Pesquisas*

Table 1
Human skin and CR-39 SSNTD atomic composition.

Element	Human skin	CR-39 detector
Hydrogen	61.7%	49.7%
Carbon	13.0%	32.4%
Oxygen	23.1%	17.9%
Nitrogen	2.0%	0%
Others	0.2%	0%

Fotovoltaicas (Photovoltaic Research Laboratory) located at DFA/IFGW/Unicamp.

Several boron thin films of different thicknesses were deposited (Table 2). They were coupled with CR-39 sheets with 1 cm^2 and then irradiated for 10 min with neutrons (flux $\sim 10^8 \text{ cm}^{-2} \text{ s}^{-1}$) at the *BNCT Beam Hole* at the IEA-R1 nuclear reactor located at IPEN/CNEN, São Paulo. Thorium and uranium thin films coupled with muscovite mica, used as neutron monitors (Bigazzi et al., 1993, 1995a, 1995b, 1999; Iunes et al., 2004), were irradiated together with the boron thin films for calibrating the CR-39 and boron thin film, respectively. The thorium monitor is based on the reaction $^{232}\text{Th}(n_{\text{fast}}, f)$ while the uranium monitor is based on the reaction $^{235}\text{U}(n, f)$.

After irradiation, the CR-39 sheets were chemically etched in a 6.25 M NaOH solution at $70 \text{ }^\circ\text{C}$ to enable the observation of the tracks at an optical microscope. In this work, the detectors were etched for a shorter time (compared to the standard time) due to the high track density ($\sim 10^6 \text{ cm}^{-2}$). The detectors labeled as "1", "2" and "3" were etched for 30 min and the detector labeled as "4" was etched for 100 min (Table 2). For the counting of tracks (on CR-39 detectors), it was used the *Zeiss Axioplan 2 Imaging Microscope* with a nominal magnification of $1000\times$. Muscovite mica plates were etched in a 48% HF chemical solution for 90 min at $15 \text{ }^\circ\text{C}$ and the track counting was performed at the *Leitz Dialux 20 EB Microscope* with a nominal magnification of $500\times$.

3. Results

3.1. Boron thin film spatial homogeneity

For the analysis of the spatial homogeneity of the boron thin films, the detectors were observed at the microscope and the tracks were counted and arranged in a matrix representing the tracks per field (spatial distribution of the tracks observed in the detector). With these counts a two-dimensional histogram was plotted and fitted with a plan function, whose only free parameter is its height (the number of tracks in the field). An example of these histograms is shown in Fig. 2. The plan function was chosen because it is desired that the boron thin films are spatially homogeneous; therefore the χ^2 -test was applied for evaluating this homogeneity. With the χ^2 and number of degrees of freedom of each distribution, the P -value was calculated and the results are shown in Table 2. Films are considered uniform if P -value ≥ 0.05 .

3.2. CR-39 calibration

For the evaluation of the fast neutron component of the flux, it is necessary to calibrate CR-39 and, for this purpose, a thorium thin film previously calibrated (Iunes et al., 2004) is used. The reactions of neutrons with the CR-39 will be induced by fast neutrons (Durham et al., 1989; Deevband et al., 2011). The same is true for ^{232}Th . The fission-track density in the muscovite coupled with the thorium thin film, $\rho_{\text{Th-232}}$, is given by:

$$\rho_{\text{Th-232}} = N_{\text{Th-232}} \epsilon_{\text{Th-232}} \int_0^{\infty} \frac{d\sigma^{\text{Th-232}}(E)}{dE} \varphi(E) dE \quad (1)$$

where the track density was determined to be $\rho_{\text{Th-232}} = (1.57 \pm 0.06) 10^3 \text{ cm}^{-2}$, the number of thorium atoms in the thin film is $N_{\text{Th-232}} = (1.570 \pm 0.058) 10^{17} \text{ cm}^{-2}$ (Iunes et al., 2004) and the fission track detection efficiency $\epsilon_{\text{Th-232}} = 1$ (muscovite mica detection efficiency; Bigazzi et al., 1995a,b). The integral of the product between differential cross section and the neutron fluence per neutron energy can be approximated by $\sigma_{\text{fast}}^{\text{Th-232}} \varphi_{\text{fast}}$ and Equation (1) becomes:

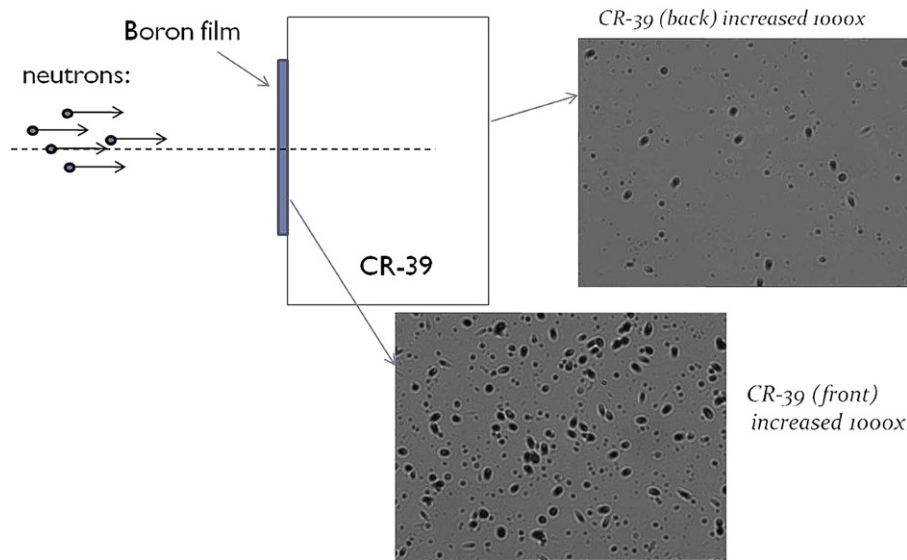


Fig. 1. Experimental assembly used during neutron irradiation (CR-39 SSNTD coupled to boron thin film) and images of the tracks revealed after chemical etching – tracks from the reactions with the detector itself (CR-39 back) and tracks from the reactions with the boron thin film (CR-39 front).

$$\rho_{\text{Th-232}} = N_{\text{Th-232}} \sigma_{\text{fast}}^{\text{Th-232}} \varphi_{\text{fast}} \quad (2)$$

from which the fluence of incident fast neutrons, φ_{fast} , is calculated:

$$\varphi_{\text{fast}} = (1.67 \pm 0.09) \cdot 10^{10} \text{ neutrons} \cdot \text{cm}^{-2}$$

For the track density in CR-39, $\rho_{\text{CR-39}}$:

$$\rho_{\text{CR-39}} = \sum_i N_{\text{CR-39}}^i \epsilon_{\text{CR-39}}^i \int_0^\infty \frac{d\sigma_i^{\text{CR-39}}(E)}{dE} \varphi(E) dE \quad (3)$$

where the index i stands for all the possible reactions occurring between neutrons and the three elements present in the detector composition (C, H and O). $N_{\text{CR-39}}^i$ stands for the number of atoms of a certain element i present in the detector and $\epsilon_{\text{CR-39}}^i$ is defined as the detection efficiency for the element i .

Assuming that the cross sections for induced fission of ^{232}Th and reactions with CR-39 do not vary significantly, the integral is approximated to $\sigma_{\text{CR-39}}^i \varphi_{\text{fast}}$ and the calibration constant $K_{\text{CR-39}}$ is defined as:

$$K_{\text{CR-39}} = \sum_i N_{\text{CR-39}}^i \epsilon_{\text{CR-39}}^i \sigma_{i,\text{fast}}^{\text{CR-39}} \quad (4)$$

With this method of calibration we obtain a general constant for the CR-39 without the need of separating each one of the reactions contributing to the track density:

Table 2

Characteristics of each boron thin film manufactured by sputtering deposition. The total track density corresponds to all the tracks observed at the CR-39 detector (tracks both from the neutrons reactions with the detector itself and the boron thin film). The label “1” corresponds to the boron thin film deposited with sputtering for 5 min, the label “2” corresponds to a 15 min sputtering deposition, the label “3” corresponds to 25 min sputtering deposition and the label “4” to 30 min sputtering deposition.

Assembly	Deposition interval time (min)	Total track density (10^6 cm^{-2})	P -value
1	5	0.46 ± 0.01	0.01
2	15	1.68 ± 0.02	0.31
3	25	2.56 ± 0.03	0.18
4	30	6.30 ± 1.51	0.90

$$K_{\text{CR-39}} = \frac{\rho_{\text{CR-39}}}{\varphi_{\text{fast}}} \quad (5)$$

Note that the cross sections for the interactions of incident neutrons with the detector itself are embraced by the calibration constant. The track densities shown in Table 3 for the CR-39 ($\rho_{\text{CR-39}}$) are obtained from the counting of tracks at the detector side that was not coupled to the boron thin film during the neutron irradiation, that is, the tracks are only due to the fast neutron reactions with the detector components.

3.3. Boron thin films calibration

In the same way, for the boron thin film calibration, it is necessary to use a previously calibrated thin film, but at this time, a uranium one, since the main contribution for the neutron capture and induced fission reactions with boron and uranium, respectively, comes from thermal neutrons.

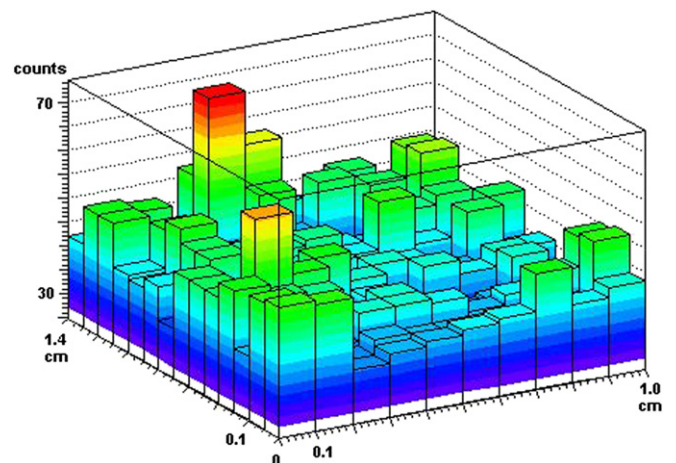


Fig. 2. Example of two-dimensional histogram of etch-pit density of all the tracks observed in the detector. In this case, the boron thin film coupled to the CR-39 detector was deposited for 15 min and its homogeneity analysis (plan fit) gives P -value = 0.31.

Table 3
Tracks densities obtained at the CR-39 SSNTDs (only due to the reactions of neutrons with the detector itself), with the corresponding calibration constants K_{CR-39} obtained from each assembly, and tracks densities obtained for only the boron reactions contribution, with the corresponding calibration constants K_B . The label “1” corresponds to the boron thin film deposited with sputtering for 5 min, the label “2” corresponds to a 15 min sputtering deposition, the label “3” corresponds to 25 min sputtering deposition and the label “4” to 30 min sputtering deposition. The resulting $^{10}B(n,\alpha)^7Li$ reaction rate measured is $R_B = (2.15 \pm 0.16) 0.10^{-10}$ decay per ^{10}B nucleus.

Assembly	CR-39 detector tracks density (10^5 cm^{-2})	CR-39 detector calibration constant, K_{CR-39} (10^{-6})	Boron thin film tracks density (10^6 cm^{-2})	Boron thin film calibration constant, K_B (10^{15} cm^{-2})
1	0.97 ± 0.02	5.81 ± 0.33	0.36 ± 0.01	1.69 ± 0.07
2	1.05 ± 0.02	6.29 ± 0.36	1.57 ± 0.02	7.30 ± 0.30
3	0.87 ± 0.02	5.21 ± 0.30	2.47 ± 0.03	11.48 ± 0.47
4	1.57 ± 0.59	9.40 ± 3.57	6.14 ± 1.51	28.53 ± 7.11

More specifically, for the uranium thin films, the neutron energies that will induce fission are mainly thermal with a contribution of epithermal through the reaction $^{235}U(n,f)$. Fast neutrons will induce fission mainly in the ^{238}U isotope. Thus, the density of fission tracks, ρ_U , determined by the muscovite coupled to the uranium film is given by (the index j stands for these two isotopes):

$$\rho_U = \sum_{j=1}^2 N_U^j \epsilon_U^j \int_0^\infty \frac{d\sigma_j^U(E)}{dE} \varphi(E) dE \quad (6)$$

$$\begin{aligned} \rho_U &= \rho_{U-235} + \rho_{U-238} \\ &= N_{U-235} \epsilon_{U-235} \int_0^\infty \frac{d\sigma_{235}^U(E)}{dE} \varphi(E) dE \\ &\quad + N_{U-238} \epsilon_{U-238} \int_0^\infty \frac{d\sigma_{238}^U(E)}{dE} \varphi(E) dE \end{aligned} \quad (7)$$

with $\epsilon_{235} = \epsilon_{238} = 1$ (muscovite mica detection efficiency). So, to calculate the fluence of incident thermal neutrons (φ_{thermal}), we must note that ^{238}U will undergo fission only in interactions with fast neutrons, while the fast neutron ^{235}U fission will be negligible compared with thermal and epithermal neutron fission events. Thus, the thermal neutron fluence can be calculated by:

$$\varphi_{\text{thermal}} \approx \frac{1}{\sigma_{\text{thermal}}^{U-235}} \left(\frac{\rho_U - N_{U-238} \sigma_{\text{fast}}^{U-238} \varphi_{\text{fast}}}{N_{U-235}} - I_{\text{epithermal}}^{U-235} \varphi_{\text{epithermal}} \right) \quad (8)$$

In Equation (8), N_{U-238} is equal to $0.9928 N_U$ (natural abundance of ^{238}U isotope is 99.28%), and the epithermal neutron contribution for the ^{235}U fission was approximated to $(N_{U-235} I_{\text{epithermal}}^{U-235} \varphi_{\text{epithermal}})$, in which $I_{\text{epithermal}}^{U-235}$ is a resonance integral. The surface concentration of uranium atoms was previously determined, $N_U = (5.96 \pm 0.14) 10^{16} \text{ cm}^{-2}$.

For the IEA-R1 nuclear reactor, in a different position of irradiation (approximately 10 cm apart from our irradiation position), it was measured (using gold foil) that the epithermal component is approximately 25% of the thermal one. Therefore, keeping this proportion for our calculations, using the density of fission tracks determined in the muscovite coupled with the uranium film, $\rho_U = (1.61 \pm 0.05) 10^4 \text{ cm}^{-2}$, and the fluence of incident thermal neutrons was found to be $\varphi_{\text{thermal}} = (5.60 \pm 0.22) 10^{10} \text{ neutrons cm}^{-2}$.

Likewise, for the boron thin films:

$$\rho_B = N_B \epsilon_B \int_0^\infty \frac{d\sigma^B(E)}{dE} \varphi(E) dE \quad (9)$$

$$\rho_B = N_B \epsilon_B \sigma_{\text{thermal}}^B \varphi_{\text{thermal}} \quad (10)$$

since the main contribution comes from thermal neutrons (the boron capture cross section for thermal neutrons is much higher than for the epithermal ones, and also the thermal component of the incident neutron flux is greater than the epithermal component). The calibration constant for the boron thin films can be defined as:

$$K_B = N_B \epsilon_B \quad (11)$$

$$K_B = \frac{\rho_B}{\sigma_{\text{thermal}}^B \varphi_{\text{thermal}}} \quad (12)$$

The results are calculated using the tracks densities for each one of the boron thin films. These track densities are obtained from the total track density (shown at Table 3) minus the background track density for the CR-39 detector (shown at Table 3), which results in tracks due to only the reactions of neutrons with the boron thin film. The value of the thermal neutron fluence is the one calculated above through uranium thin films. The results are shown in Table 3.

It is also possible to estimate the thickness of each boron thin film from the number of tracks due only to the reactions of neutrons with the boron thin film, i.e., using the calibration constant K_B , which gives the superficial density of the boron atoms present the thin film. For this, it is necessary to know the approximate composition of the film, which will provide its volumetric density, from which it is possible to estimate the thin film thickness. For the manufactured boron thin films, an analysis with XPS (X-ray Photoelectron Spectroscopy) reveals that their atomic composition is approximately 85% of boron atoms and 15% of oxygen atoms and assuming that all the oxygen is bounded with boron in the form of boron trioxide (B_2O_3), the thin films thicknesses are of about 0.9 nm (for the 5 min sputtering deposition) to 14.5 nm (for the 30 min deposition).

Other methods for estimating the thickness such as profilometer and atomic force microscope (AFM) were used but none of these devices were able to determine the boron thin film thicknesses. The fact that the film thickness is smaller than the resolution of these devices means that the goal of this work (making a film that is much thinner than the range of the particle) has been reached.

3.4. $^{10}B(n,\alpha)^7Li$ reaction rate measurement

After calibrating the boron thin films, the method can be applied to calculate the reaction rate of interest in BNCT.

Defining the reaction rate as:

$$R_B = \int_0^\infty \frac{d\sigma^B(E)}{dE} \varphi(E) dE \quad (13)$$

it is possible to rewrite it as

$$R_B = \frac{\rho_B}{K_B} \quad (14)$$

and from the calibration constants K_B found for each boron thin film (shown at Table 3), the reaction rate found for the irradiation with neutrons (for 10 min) is $R_B = (2.15 \pm 0.16) 0.10^{-10}$ decay per ^{10}B nucleus.

4. Discussions and conclusions

When choosing the thin film deposition via sputtering method, considerations and cautions regarding the experimental apparatus and work objective must be taken. If a very thin film is needed, the deposition will be performed for a short time and the probability of obtaining a non homogeneous film is greater since when the atoms are ejected from the target and are deposited onto the substrate, the island growth is a critical stage (these island structures indicate the tendency to form continuous thin films). This is the most likely cause for the lack of areal homogeneity presented by boron thin film “1”. As said at the methodology section, CR-39 sheet coupled to the boron thin film “4” was chemically etched during a longer time (100 min) compared to the sheets coupled to the other boron thin films (30 min). Thus, the surface etch pit density is increased because more tracks are etched (higher etching efficiency is expected). In addition, etch pit diameters are also increased. The net result of the combination of these two factors is that a greater area of the detector is covered by etch pits. In our case, we observed that a considerable amount of tracks overlapped, causing an additional difficult in counting them. Therefore, taking into account the track densities involved in the intended measurements, it is preferable to work in this under-etching condition (30 min). This is still a point of the etching curve (etch pit density versus etching time), in which the density is linearly increased with etching time, demanding a greater control in etching temperature and reagent concentration.

The calibration method for the CR-39 SSNTD and the boron thin film assumes certain hypothesis regarding the interactions of neutrons of different energies with the elements in consideration since the energy spectrum of the irradiation position used for the irradiations is still not so well characterized. For the approximations, the neutron spectrum energy is divided in three regions (thermal, epithermal and fast) and the contributions for the calibrations are analyzed considering the reactions cross sections. For the CR-39 calibration, it is considered (Durham et al., 1989; Deevband et al., 2011) that only fast neutrons will induce reactions at the detector and that the thermal and epithermal neutrons do not induce fissions on ^{232}Th (based on the cross section analysis). For the boron thin film calibration, first of all, it is necessary to make assumptions about the interactions of $n + \text{U}$ (i.e. only thermal and epithermal neutrons will significantly induce fissions on ^{235}U and only fast neutrons will contribute to reactions with ^{238}U) and the relative contribution of the thermal and epithermal components of the neutron beam at the reactor. Again, the cross sections must also be analyzed.

The calibration factors determined in this work depend upon etching and observation efficiencies. For the thin films, depend also on their boron concentrations and therefore on their thicknesses. It was not possible to estimate the boron thin films thicknesses using a profilometer or an atomic force microscope (AFM) since the quantity of boron atoms deposited in each film was too small. The XPS analysis shows also some presence of iron atoms which is probably due to the stainless steel substrate, i.e., there are probably some parts of the substrate that were not covered with boron atoms (formation of atomic islands in the thin film growth process), corroborating the fact that the films manufactured are very thin.

For CR-39, the calibration factors depend on its density and atom composition. In either case the calibration factor is specific for

the laboratory protocol to determine track density. However, once determined the calibration factors, it is possible to determined boron reaction rate and the fast neutron contribution for the flux, just measuring track densities on the side of the CR-39 sheet coupled with the film and on the side that has not been coupled with it.

As it was expected, the results for the CR-39 calibration constants ($K_{\text{CR-39}}$) are approximately equal and the discrepancies can be due to the different etching times and solution concentration applied. It must be noted that ideally the detectors have to be etched together to avoid different etch conditions. In this work the detectors were etched separately and since the time intervals chosen for the etching process were much smaller than the standard one (400 min), any small difference in time and solution concentration will interfere greatly in the final result. Besides that, the neutron flux used for the irradiations is not homogeneous: there is a flux gradient on the axis perpendicular to the assemblies (Fig. 1) and any difference in the irradiation position of the setup can interfere in the quantity of induced events.

It has been shown that, using the sputtering method, it is possible to produce homogeneous films suitable for the measurement of the $^{10}\text{B}(n,\alpha)^7\text{Li}$ reaction rate. In a previous work (Smilgys et al., 2011, in press), it was shown that it is also possible to produce such homogeneous films using the Chemical Deposition Method to deposit a boron-based solution on a mica plate. The main advantage of the sputtering is that it allows for the manufacturing of thinner films, which can be used to monitor higher fluence irradiations. For the fluencies normally used in BNCT studies, 10^{12} neutrons/cm² (Coderre and Morris, 1999; Barth et al., 2005), the films manufactured by both methods work well, although with a weaker etching (compared to our standard).

The report number 86 of the International Commission on Radiation Units and Measurements (ICRU, 2011) brought to attention that in cases where the effects of radiation can be considered inhomogeneous (when there is less than one event per cell), the average dosimetric quantities, such as absorbed dose, are not appropriate to describe radiation damage in association with biological effects and recommended to calculate the particle radiance, which is the energy and direction-dependent number of emitted particles, to describe this inhomogeneous fraction of the dose. BNCT is planned to match the homogeneity requirement of one event per cell, in the tumor. However, there are also three other high LET secondary sources of dose (the first is the boron in health tissue and blood; the second is the proton emission from the $^{14}\text{N}(n,p)^{14}\text{C}$ reaction; the third is the eventual contamination of the neutron flux by fast neutrons, which will interact with the atoms compounding human tissue, producing mainly energetic protons) that have to be treated as producing inhomogeneous radiation effects.

The use of CR-39 for BNCT purposes is promising, not only because of its ability of monitoring fast neutrons, but also because its atom composition ($\text{C}_{12}\text{H}_{18}\text{O}_7$) is very similar to the tissue one. The density of tracks from products of the fast neutron reactions detected by CR-39 is proportional to the proton radiance and can be evaluated at the micrometer scale. Thus, CR-39 is a potential candidate for microdosimetric studies (as a tissue-equivalent material) of the inhomogeneous component of BNCT irradiation doses. In addition, the products of the $^{10}\text{B}(n,\alpha)^7\text{Li}$ reaction are also directly detected allowing for the determination of this reaction rate.

Acknowledgments

We would like to thank CAPES/CNPq for the financial support.

References

- Altieri, S., Bortolussi, S., Bruschi, P., Chiari, P., Fossati, F., Stella, S., Prati, U., Roveda, L., Zonta, A., Zonta, C., Ferrari, C., Clerici, A., Nano, R., Pinelli, T., 2008. Neutron autoradiography imaging of selective boron uptake in human metastatic tumours. *Appl. Radiat. Isot.* 66, 1850–1855.
- Barth, R., Coderre, J.A., Vicente, M.G.H., Blue, T.E., 2005. Boron neutron capture therapy of cancer: current status and future prospects. *Clin. Cancer Res.* 11, 3987–4002.
- Behrisch, R., 1981. *Sputtering by Particle Bombardment I: Physical Sputtering of Single-Element Solids*. Springer, Berlin, ISBN 3540105212.
- Bigazzi, G., Hadler, J.C., Lunes, P.J., 1993. Mineral dating by the fission track method: neutron dosimetry by thin film of natural uranium. *Revista de Física Aplicada e Instrumentação* 8, 13–23.
- Bigazzi, G., Hadler, J.C., Lunes, P.J., Mello, T.C.W.P., Navia, L.M.S., Paulo, S.R., Zúñiga, A., 1995a. Employment of thin thorium films in fission track neutron dosimetry. *Braz. J. Phys.*, 246–251.
- Bigazzi, G., Hadler, J.C., Lunes, P.J., Oddone, M., Paulo, S.R., Zúñiga, A., 1995b. Absolute thermal neutron fluence determination by thin film of natural uranium. *Nucl. Instrum. Meth. Phys. Res.* A352, 588–591.
- Bigazzi, G., Guedes, S., Hadler, J.C., Lunes, P.J., Oddone, M., Osorio, A.M., Paulo, S.R., Zúñiga, A., 1999. Potentialities and practical limitations of an absolute neutron dosimetry using thin films of uranium and thorium applied to the Fission Track Method. *Radiat. Meas.* 31, 651–656.
- Coderre, J.A., Morris, G.M., 1999. The radiation biology of boron neutron capture therapy. *Radiat. Res.* 151, 1–18.
- Deevband, M.R., Abdolmaleki, P., Kardan, M.R., Khosravi, H.R., Taheri, M., 2011. An investigation on the response of PADC detectors to neutrons. *Appl. Radiat. Isot.* 69, 340–345.
- Durham, J.S., Blue, T.E., Wehring, B.W., Ragheb, M.H., Blue, J.W., 1989. Microdosimetry in fast-neutron therapy by automatic readout of CR-39 solid state nuclear track detectors. *Nucl. Instr. Meth. Phys. Res.* B36, 319–331.
- ICRU, 2011. Quantification and reporting of low-dose and other heterogeneous exposures. *J. ICRU* 11, 1–77.
- Lunes, P.J., Hadler, J.C., Bigazzi, G., Guedes, S., Zúñiga, A., Paulo, S.R., Tello, S.C.A., 2004. Uranium and thorium thin film calibrations by particle track techniques. *J. Radioanalytical Nucl. Chem.* 262, 461–468.
- Smilgys, B., Guedes, S., Hadler, J.C., Coelho, P.R.P., Alencar, I., Soares, C.J., Salim, L.A., 2011. Manufacturing of boron thin films for the measurement of the $^{10}\text{B}(n,\alpha)^7\text{Li}$ reaction in BNCT. *Proc. Sci.* XXXIV BWNP.